# Supplementary Figure 1

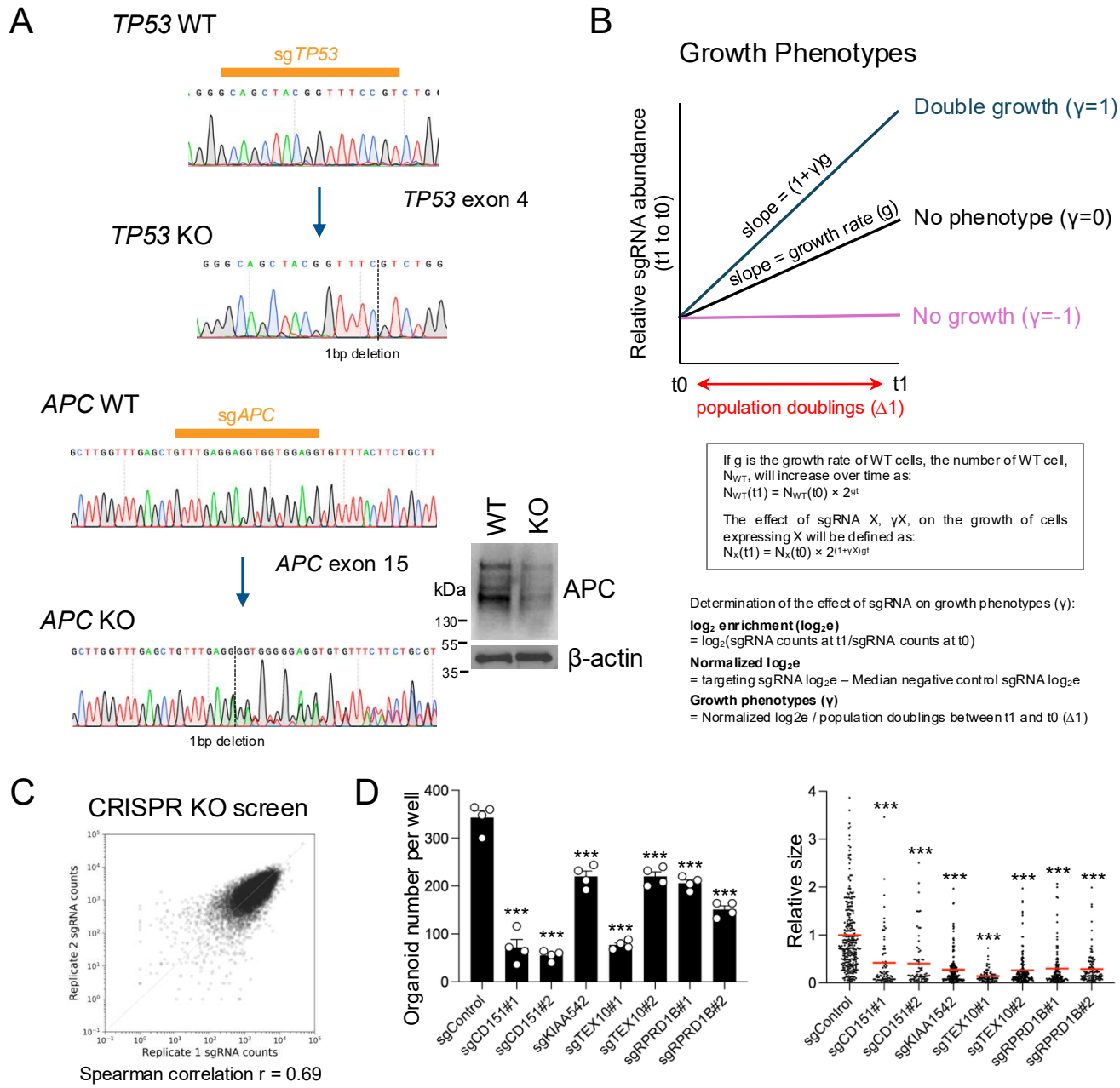


**Supplementary Figure 1. CRISPR KO screen in an oncogene-engineered *TP53/APC* DKO human gastric tumor organoid model. (A)** Sanger sequencing indicated indels that were created by CRISPR/Cas9 cleavage in normal human gastric organoids. A *TP53/APC* DKO organoid line contained indels in *TP53* exon 4 and *APC* exon 15. **(B)** Wild-type (WT) cells with a given growth phenotype have an intrinsic growth rate g. The $log_2$ enrichment ($log_2e$) of a cell population with a specific growth phenotype can be calculated by counting the abundance of individual sgRNA at the endpoint t1 versus initial time point t0. To quantify the effect (γ) of individual sgRNA on the growth rate relative to WT, $log_2e$ of a targeting sgRNA is normalized to the median $log_2e$ of the negative control sgRNA and then divided by population doublings between t1 and t0 (Δ1). Population doublings are calculated by measuring the growth of the bulk population (using standard cell quantification assays). **(C)** High correlation of sgRNA counts between two independent replicates for the CRISPR KO screen of Figure 2. **(D)** Quantification of Figure 1F. Left panel: number of organoids per well. Right panel: relative organoid size. Each dot represents an individual organoid. T-test. ***, p<0.001.

# Supplementary Figure 2

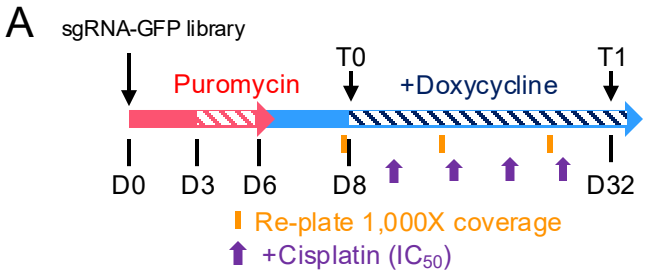


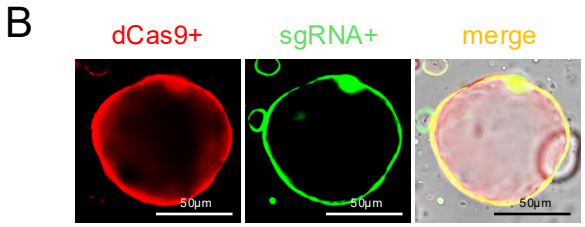


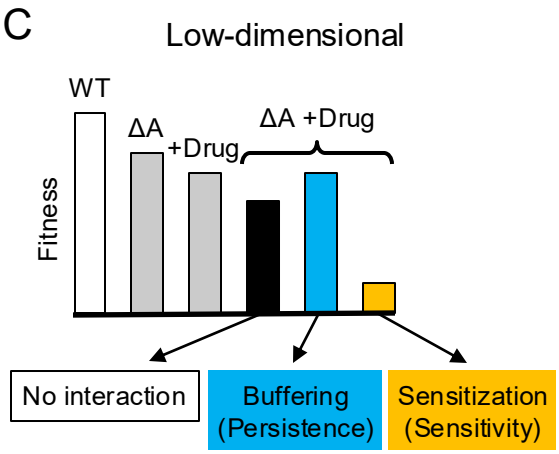


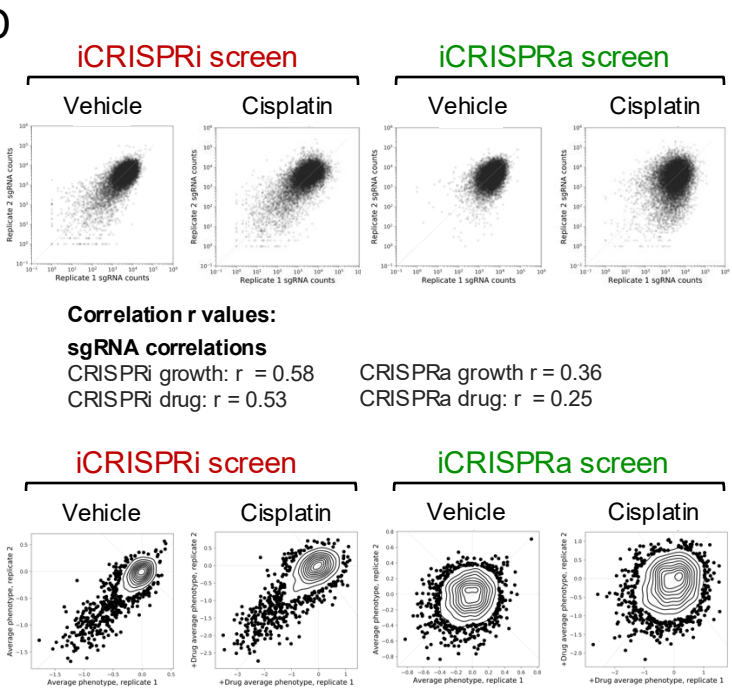


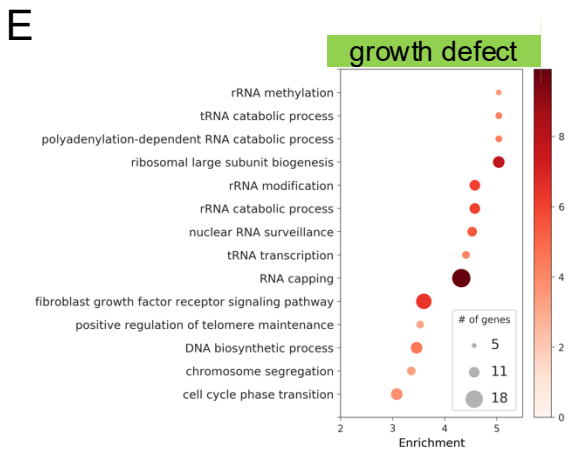


**Supplementary Figure 2. Inducible CRISPRi and CRISPRa screens in an oncogene-engineered *TP53/APC* DKO human gastric tumor organoid model. (A)** Timeline of iCRISPRi and iCRISPRa screens. **(B)** Immunofluorescence images indicated co-expression of dCas9 fusion proteins (mCherry as the reporter) and sgRNAs (GFP as the reporter) in organoids. **(C)** CRISPR screens measure one-dimensional phenotypes of epistasis (buffering or sensitization), compared to the theoretical additive model for no interactions. ΔA is gene knockdown or knockout. +Drug is the addition of drug. The y-axis is the fitness score, with a lower score meaning a lower fitness (stronger growth defect). **(D)** Correlation of sgRNA counts and genes between two independent replicates for iCRISPRi and iCRISPRa screens. **(E)** Gene ontology analyses identified top biological pathways that are significantly associated with cell growth defect phenotypes from pooled iCRISPRi screens.

# Supplementary Figure 3

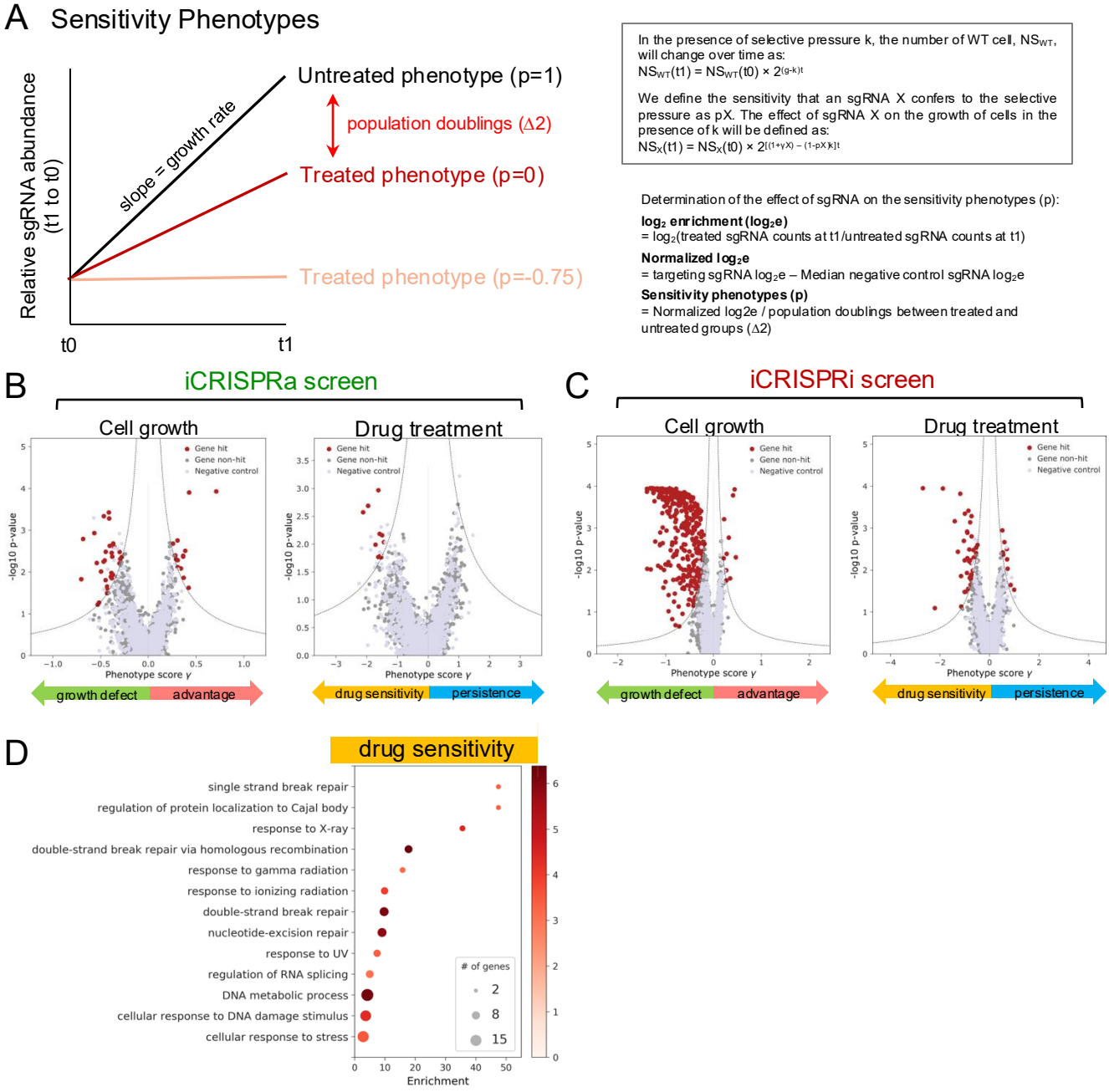


**Supplementary Figure 3. Schematic of buffering or sensitization effects. (A)** The phenotype of cells exposed to a selective pressure (e.g., cisplatin treatment) can be calculated from the $\log_2$e of treated and untreated populations. The effect of a sgRNA on sensitivity phenotype (p) is defined as a normalized $\log_2$e divided by population doublings between untreated and treated populations (Δ2). **(B)** Volcano plot summarizing cell growth and drug sensitivity phenotypes for sgRNA targets in the pooled iCRISPRa. Each dot represents a sgRNA target. Statistically significant hits (labeled in red) that are determined by Mann-Whitney U test. **(C)** Volcano plot summarizing cell growth and drug sensitivity phenotypes for sgRNA targets in the pooled iCRISPRi. Each dot represents a sgRNA target. Statistically significant hits (labeled in red) that are determined by Mann-Whitney U test. **(D)** Gene ontology analyses identified top biological pathways that are significantly associated with cisplatin sensitivity phenotypes from pooled iCRISPRi screens.

# Supplementary Figure 4

A

| sgRNA target | Cisplatin IC50 (μg/mL) |
|---|---|
| *Control* | 1.58 |
| *ERCC6* | 0.42 |
| *ERCC4* | 0.29 |
| *BRCA1* | 1.01 |
| *ELOF1* | 0.53 |
| *GTF2H5* | 0.43 |
| *LEO1* | 0.71 |
| *ZFP36L2* | 0.99 |
| *ZNF677* | 0.51 |

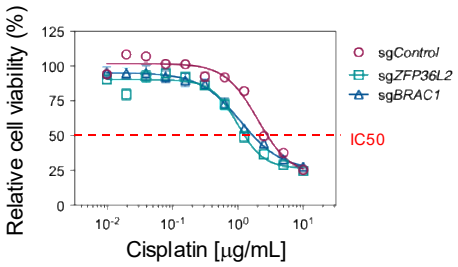


B

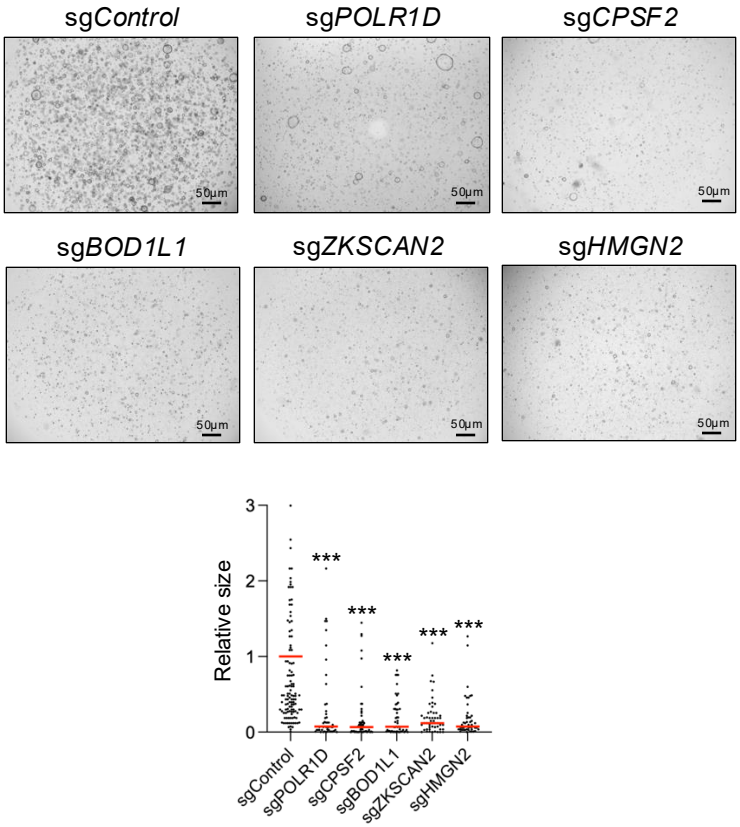


**Supplementary Figure 4. Individual validation of significant hits generated from iCRISPRi screens. (A)** A list of cisplatin $IC_{50}$ in individual iCRISPRi knockdown organoid lines. The $IC_{50}$ of *ZFP36L2* and *BRCA1* knockdown organoid lines was generated from a 12-point concentration cisplatin sensitivity assay. All dose curves utilized n=4 technical replicates. **(B)** A lentiviral construct carrying a BFP reporter was used to deliver sgRNAs into parental iCRISPRi *TP53/APC* DKO human gastric tumor organoids. After doxycycline induction, individual organoid lines were grown from 20,000 single FACS-sorted BFP+/mCherry+ cells in a Matrigel dome. Brightfield images were taken 11 days after cell sorting. Compared with control, iCRISPRi organoid lines exhibited growth defect phenotypes. Quantification of relative organoid size. Each dot represents an individual organoid. T-test. ***, p<0.001.

# Supplementary Figure 5

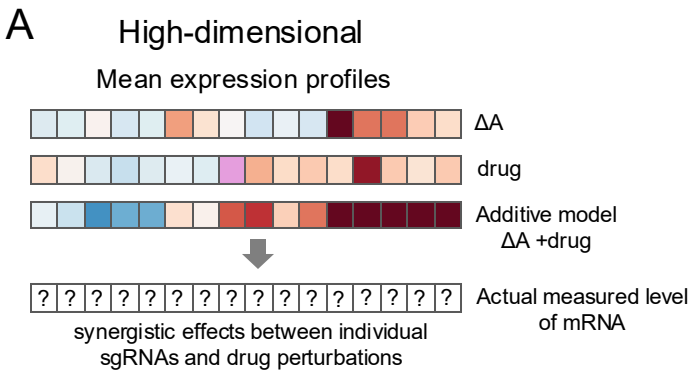


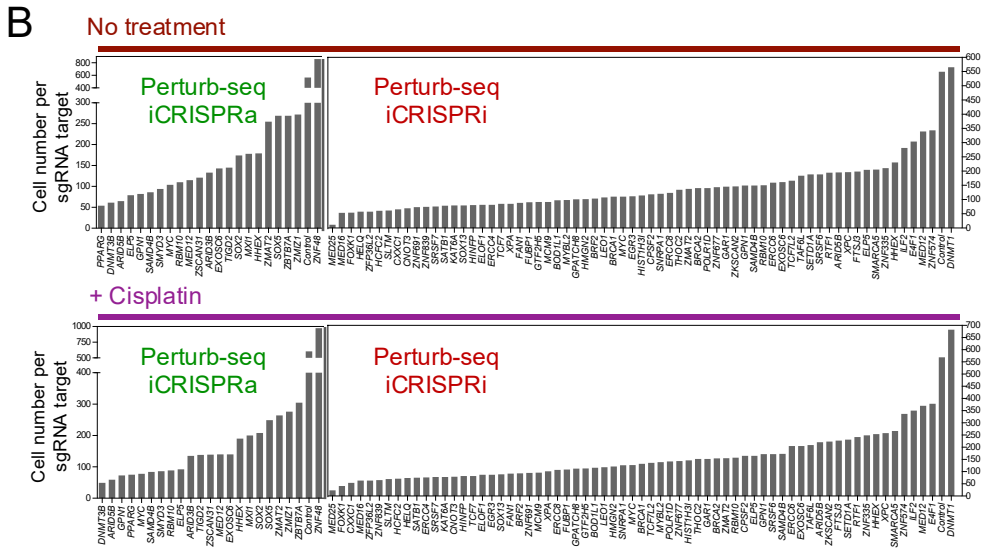


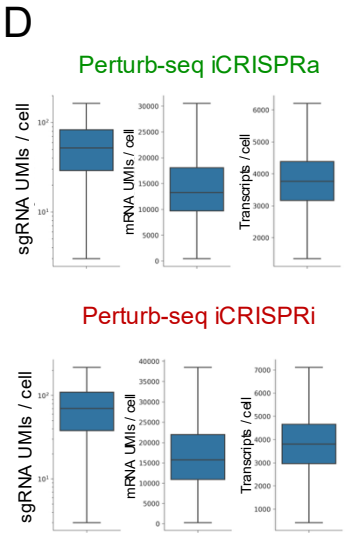


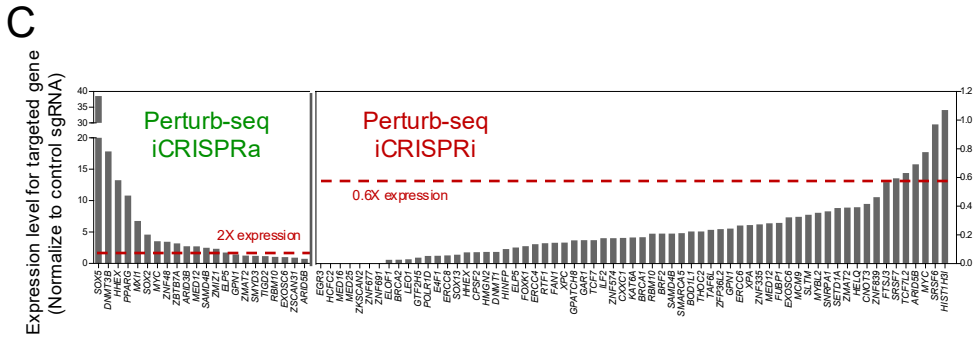


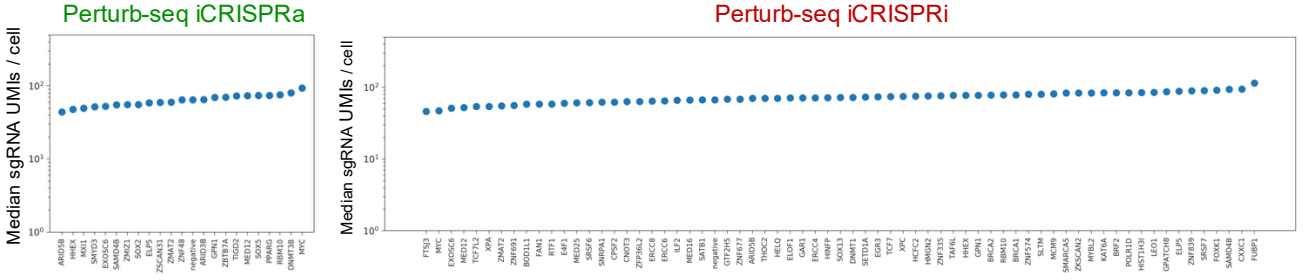

**Supplementary Figure 5. Quality control of single-cell Perturb-seq in organoids. (A)** Perturb-seq measures high-dimensional phenotypes of synergistic effects, where instead of a single fitness value measured, a high-dimensional transcriptional response is observed. Particularly, for each individual Perturb-seq sgRNA, we quantitated effects on distinct mRNA abundance after treatment with (1) sgRNA alone (ΔA, no cisplatin) or (2) cisplatin alone (drug, negative control sgRNA plus cisplatin). The theoretical sum effect of condition (1) and (2) on a given mRNA expression was predicted as a third metric (3, "additive model", ΔA +drug). For the actual measured level of mRNAs from Perturb-seq, individual genes can be further up- or down- regulated compared to the expected additive model to reveal synergistic effects between individual sgRNAs and drug perturbations. **(B)** Bar diagrams show individual Perturb-seq sgRNA targets and total cell numbers per sgRNA that were captured by iCRISPRi and iCRISPRa Perturb-seq screens. **(C)** Bar diagrams show the knockdown (iCRISPRi) and overexpression (iCRISPRa) efficiency of individual Perturb-seq sgRNA perturbation. Compared to control sgRNAs, 64 out of 69 iCRISPRi Perturb-seq sgRNAs exhibited at least a 40% decrease of average target gene expression from all cells bearing the same sgRNA, whereas 12 out of 22 iCRISPRa Perturb-seq sgRNAs showed at least of 2-fold increase of target gene expression. The mRNA level represents the average expression of all cells that express the same sgRNA. Relative mRNA level is normalized to cells with the control sgRNA. **(D)** Perturb-seq in organoids allows for robust sgRNA identity assignment and transcriptome capture. Box plots displaying the sgRNA UMIs (unique molecular identifiers) per cell, mRNA UMIs per cell, and transcripts per cell in both the iCRISPRi and iCRISPRa Perturb-seq screens. Box plots denote quartile ranges (box), median (center mark), and 1.5 × interquartile range (whiskers). **(E)** Median sgRNA UMI counts per cell (capture rate) for cells assigned to each guide identity, for both the iCRISPRi and iCRISPRa Perturb-seq screens.

# Supplementary Figure 66

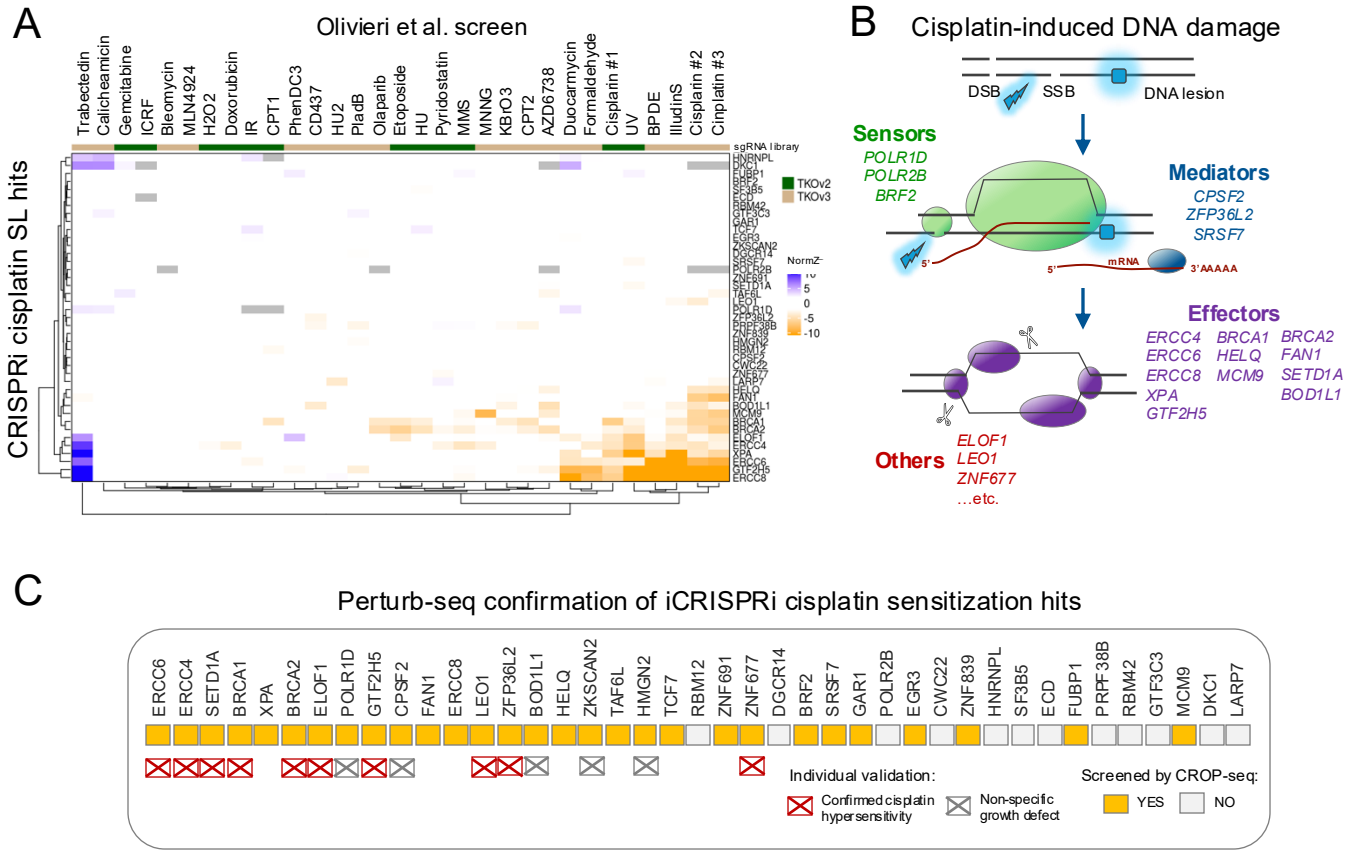


C




**Supplementary Figure 6. Top hits of iCRISPRi screens. (A)** Among top iCRISPRi cisplatin sensitization hits, many uncharacterized cisplatin sensitization partners were identified, supported by the heat map representation of gene-drug dependency from previous genome-scale CRISPR dropout screens in a 2D hTERT-immortalized RPE1 cell line (Olivieri et al.). The x-axis shows different genotoxic agents, including cisplatin, which was applied to the 2D screens of Olivieri et al.. The y-axis lists the top 41 cisplatin sensitivity hits generated from our iCRISPRi 3D screen in this study. Yellow/orange indicates drug sensitization. Purple/blue indicates drug persistence. **(B)** The iCRISPRi screen of Figure 3 revealed key components of cisplatin-induced DNA repair signaling pathways, including DNA damage sensors, mediators, and effectors, in addition to novel loc. **(C)** Summary of cisplatin sensitization hits in the primary iCRISPRi screen and hit validation.

# Supplementary Figure 7

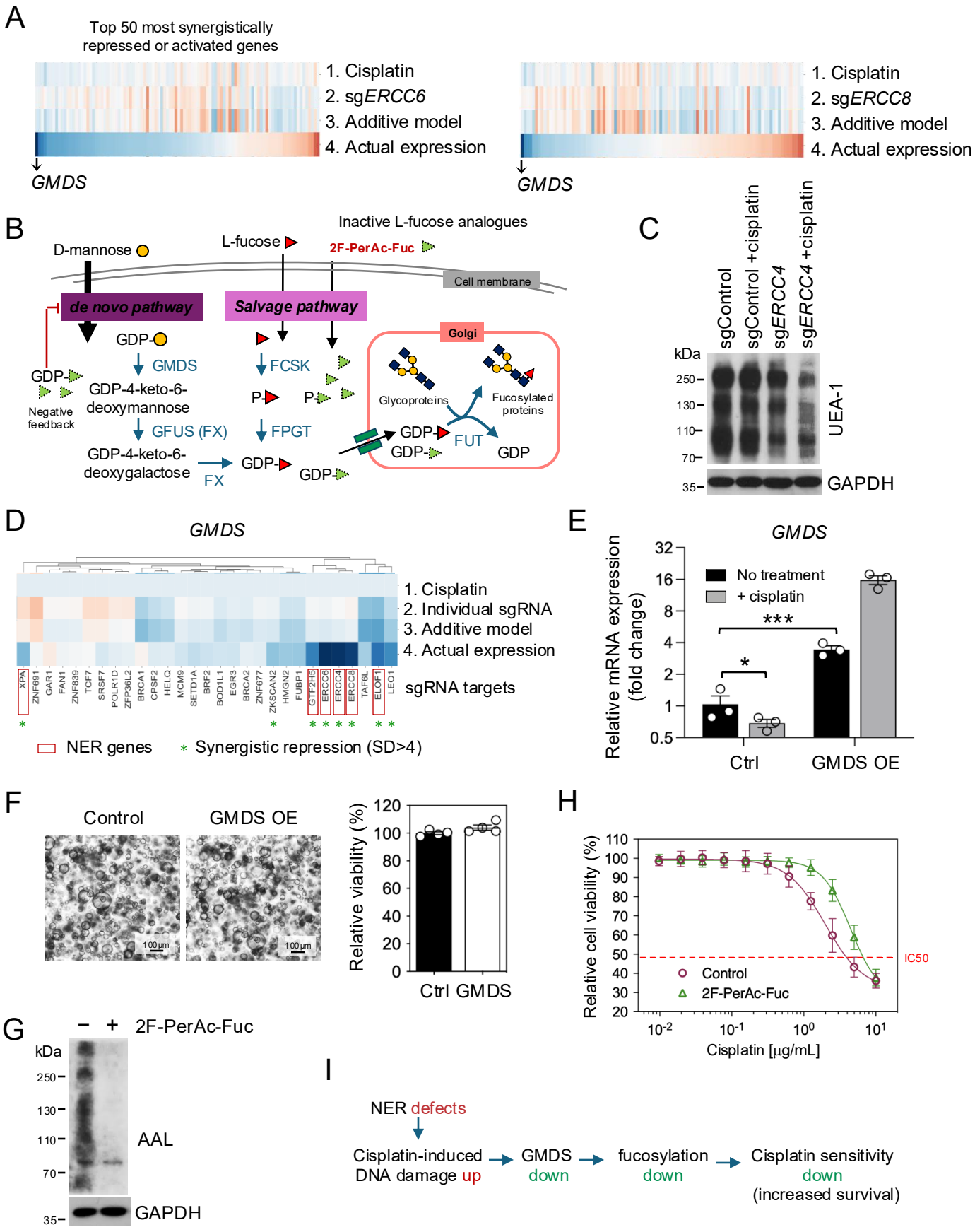

**Supplementary Figure 7. Mechanistic insights of CRISPR screens. (A)** Synergistic repression of *GMDS* in the combination of *ERCC6* or *ERCC8* knockdown and cisplatin treatment. **(B)** Schematic of fucosylation biosynthetic pathways. **(C)** Synergistic repression of fucosylated proteins by combining *ERCC4* knockdown and cisplatin treatment. Total fucosylated proteins were determined by UEA-1 Western blotting. **(D)** *GMDS* expression was assessed in each sgRNA iCRISPRi knockdown. Known NER genes are boxed in red. The knockdowns of *ERCC4*, *ERCC6*, *ERCC8*, *XPA*, *ELOF1*, *GTF2H5*, *ZKSCAN2,* and *LEO1* were unified by synergistic repression of *GMDS* expression, which was not observed in non-NER genes. The green asterisks indicate a significant deviation of *GMDS* expression between predicted (condition 3) and actual (condition 4) (>4 SD), indicating unexpected synergistic *GMDS* repression, which was again specific for NER sgRNA knockdown. **(E)** GMDS overexpression rescued cisplatin-induced GMDS repression. Organoids were treated with 2 μg/mL cisplatin for 72 hrs. Three independent experiments (N=3) were performed. The horizontal bar indicates the mean. The error bar represents SEM. **(F)** GMDS overexpression did not inhibit the growth of organoids. Brightfield images were taken for organoid growth on day 10 after passage. Four independent experiments (N=4) were performed. Quantification of metabolic activity was determined by Alamar blue assay. **(G)** Inactive L-fucose analogs 2F-PerAc-Fuc inhibited fucosylation. Total fucosylated proteins were determined by AAL Western blotting. **(H)** Pharmacologic inhibition of fucose biosynthesis using 2F-PerAc-Fuc reduced cisplatin sensitivity in organoids. A fully titrated cisplatin treatment was performed in three independent experiments (N=3). **(I)** Schematic of the working model. In response to either DNA damage induced by cisplatin alone or to the more severe stress of cisplatin and NER gene knockdown, *GMDS* repression acts as a pro-survival signal.

# Supplementary Figure 8

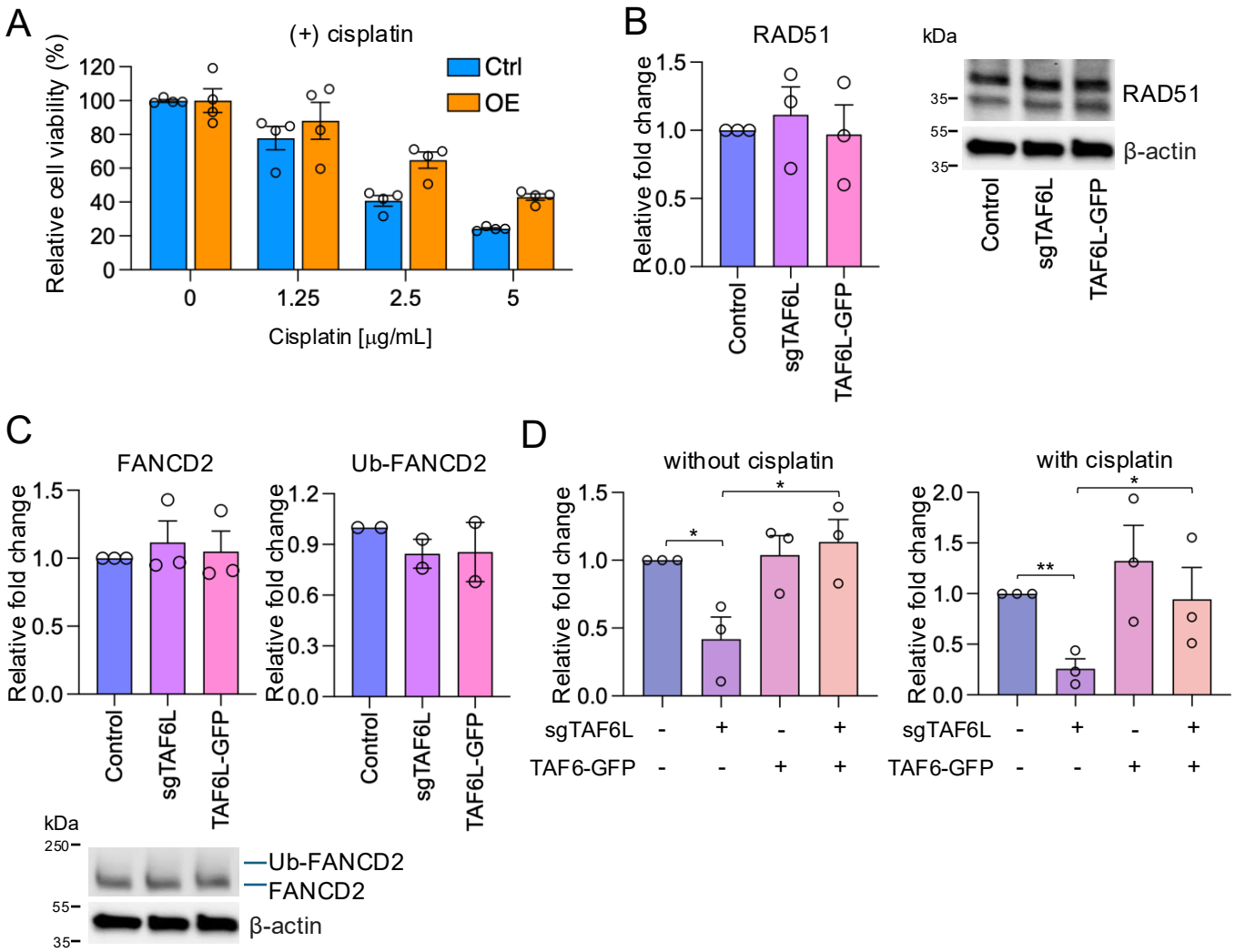


**Supplementary Figure 8. TAF6L regulates cisplatin sensitivity. (A)** Cell viability of Control (Ctrl) or *TAF6L-GFP* overexpression (OE)*TP53* KO organoids after three days of cisplatin treatment. *TAF6L-GFP* OE shows a trend of decreased sensitivity to cisplatin. Cell viability is shown from four technical replicates per condition. Data points represent one of two independently performed experiments. **(B)** TAF6L expression, whether knockdown or overexpression, did not alter RAD51 levels. RAD51 quantification was performed from three independent Western blotting experiments. **(C)** TAF6L expression, whether knockdown or overexpression, did not alter FANCD2 levels. FANCD2 quantification was performed from three independent Western blotting experiments. Ub-FANCD2 quantification was performed from two independent Western blotting experiments. **(D)** Related to Figure 6E. EdU assay in parental control, *TAF6L* KD, *TAF6L-GFP* OE, and TAF6L-GFP re-expression in *TAF6L* KD organoids. The relative fold change of EdU+ cells was normalized to the control with or without cisplatin treatment. Quantification based on three independent experiments was shown (N=3). T-test. *, $p<0.01$.

# Supplementary Figure 9

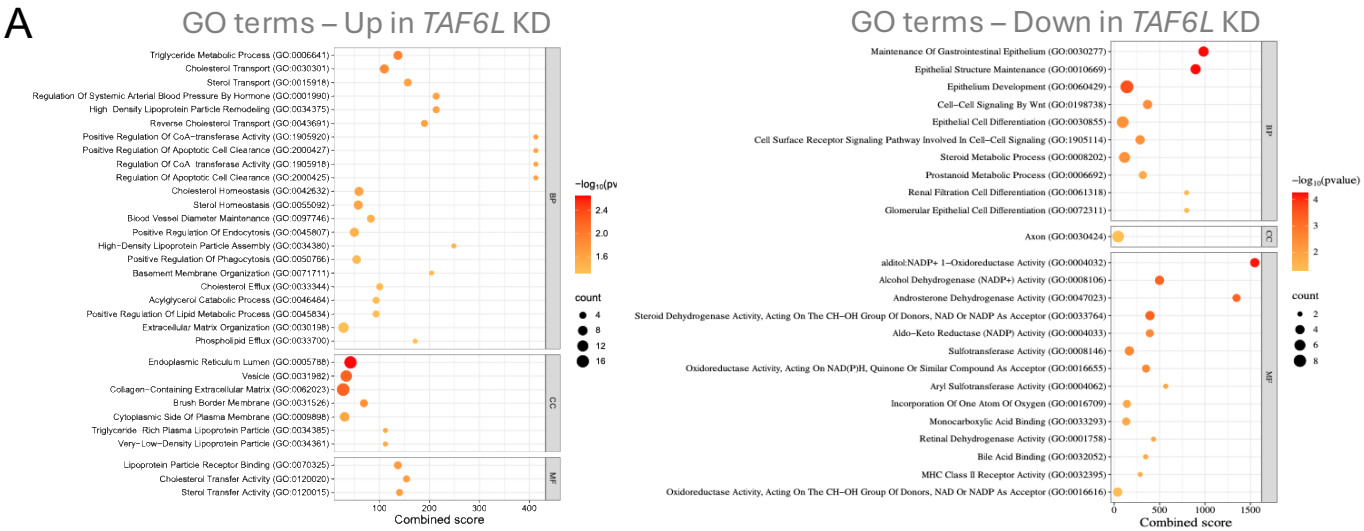


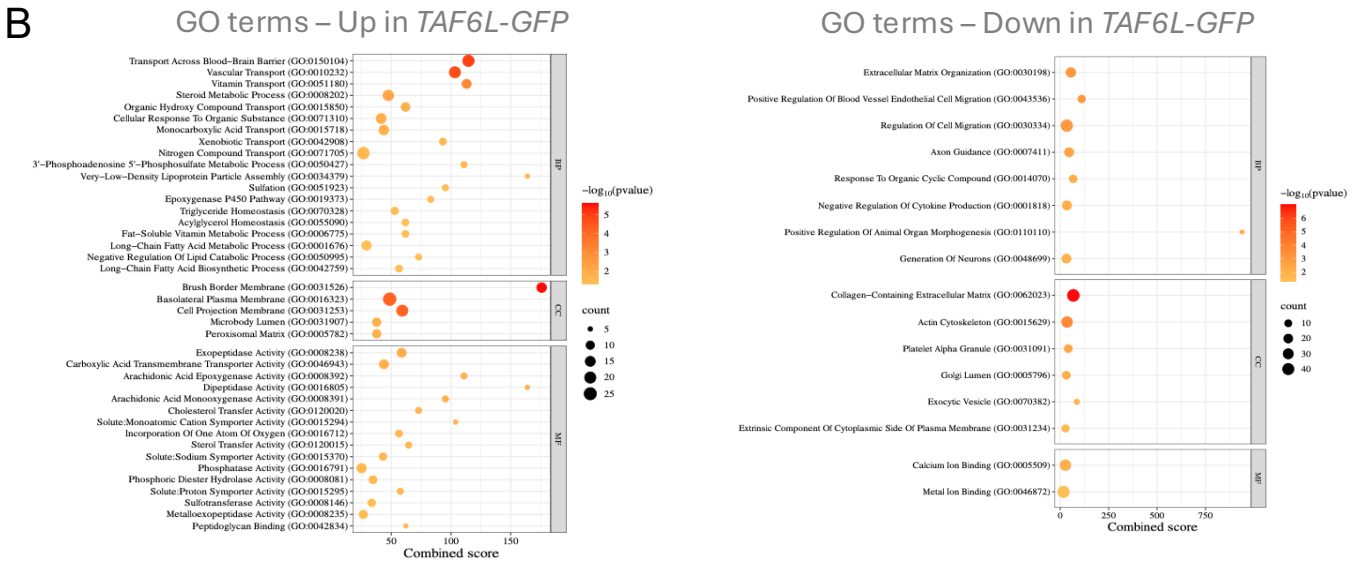


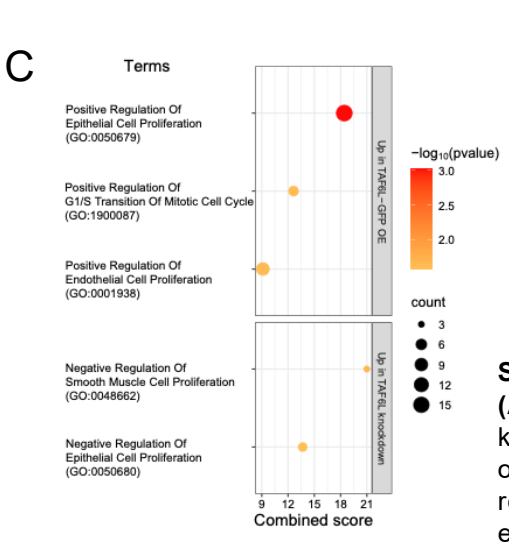


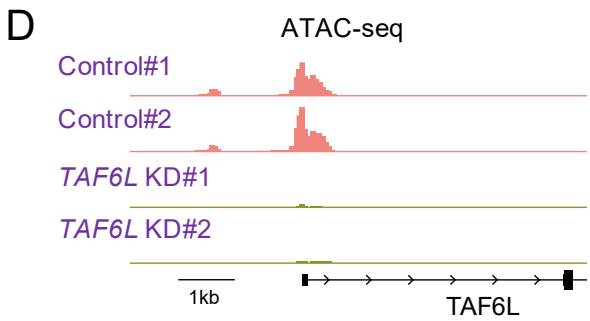


**Supplementary Figure 9. TAF6L-associated biological processes.** **(A)** GO analysis using Enricher identified ontology terms in *TAF6L* knockdown organoids. **(B)** GO analysis using Enricher identified ontology terms in *TAF6L-GFP*-expressing organoids. **(C)** GO terms related to cell proliferation were identified using differential gene expression generated by RNA-seq, showing that *TAF6L-GFP* OE enhances cell proliferation while *TAF6L* KD inhibits it. **(D)** ATAC peaks were significantly downregulated at the promoter regions of *TAF6L*.

# Supplementary Figure 10

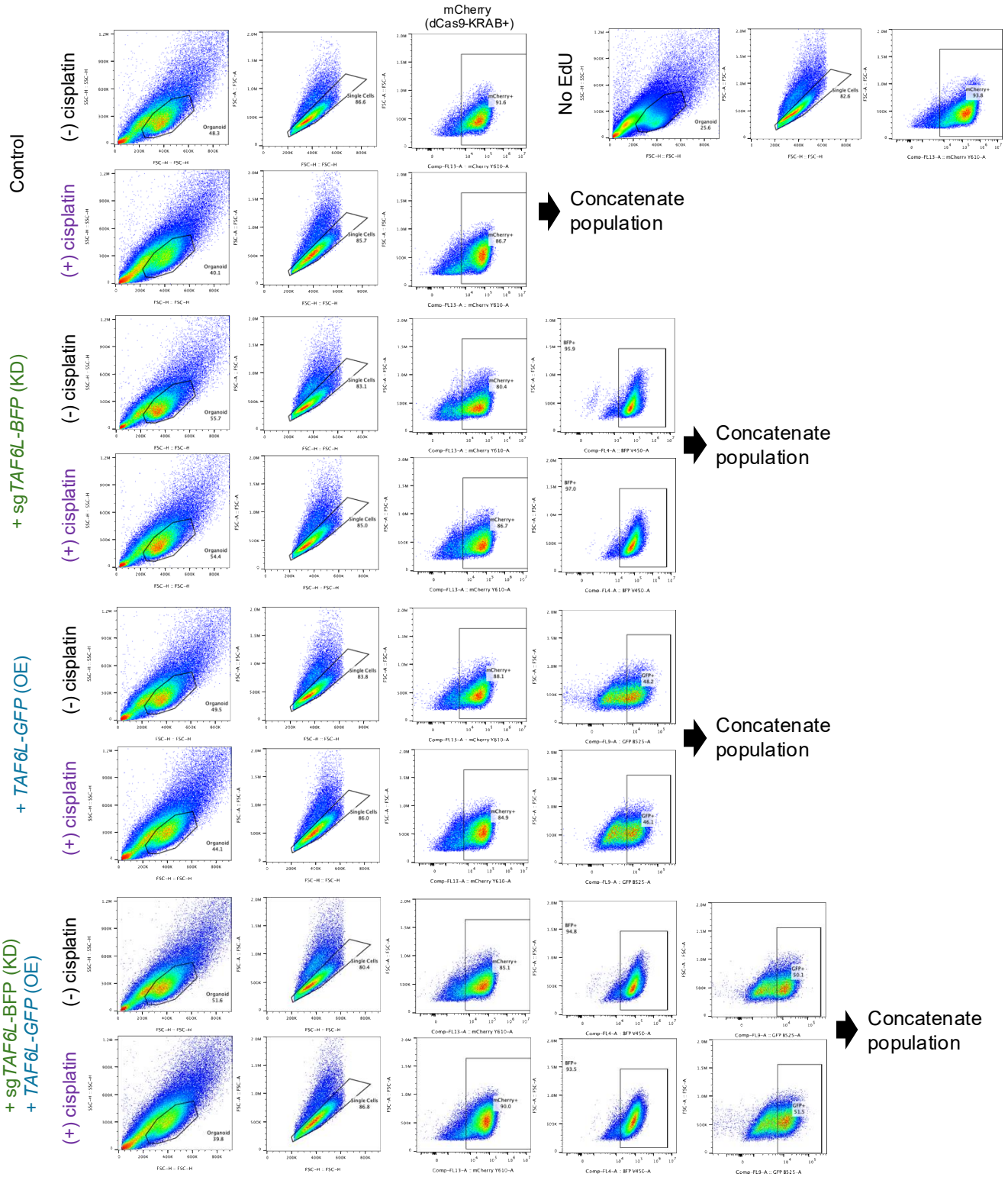


**Supplementary Figure 10. FACS gating strategy related to Figure 6E.** Single cells were first gated, and then cells expressing dCas9-KRAB (mCherry+) were further separated based on the presence of *TAF6L* sgRNA (BFP+) and TAF6L-GFP (GFP+) to distinguish *TAF6L* knockdown and *TAF6L* overexpression populations. EdU incorporation was subsequently used to determine the proportion of proliferating cells within these different populations.